Non-Equilibrium Parameter for a Hybrid Fokker-Planck / DSMC Scheme

Christian Hepp, Martin Grabe and Klaus Hannemann

German Aerospace Center (DLR), Bunsenstraße 10, D-37073 Göttingen, Germany

Corresponding author: Christian.Hepp@dlr.de

Abstract. In this work we investigate the kinetic Fokker-Planck (FP) model [1, 2] concerning its applicability to simulate hypersonic, rarefied gas flow. As in the direct simulation Monte Carlo (DSMC) algorithm, the FP model simulates the stochastic motion of a set of particles through the computational domain which results in a simple coupling of both methods. No collisions must be calculated in the FP approach and so larger cell and time step sizes than by DSMC calculations can be used. Because of this, the FP model holds the potential to be more efficient than DSMC where the Knudsen number is small. Further we present and investigate a hybridisation scheme for the FP and DSMC algorithms. We derive a non-equilibrium parameter from the Fokker-Planck- and Boltzmann-operator which indicates the validity of the FP model. In hybrid simulations this parameter is used to partition the computational domain in DSMC and FP regions. The particle motion is processed similarly in both regions, only the procedure for assigning new particle velocities differs. To achieve an equal number of particles per cell, weighting factors depended on the cell size are used. The hybridisation scheme is tested for one-dimensional shock and two-dimensional cylinder flows and gives results in agreement to pure DSMC simulations. An efficiency study shows, that the hybrid scheme is roughly five times faster than a pure DSMC simulation for a hypersonic cylinder flow test case.

INTRODUCTION

Numerical simulation of hypersonic rarefied gas flows requires modelling of non-equilibrium flow phenomena, such as shock waves. While strong non-equilibrium effects can not accurately be modelled by the Navier-Stokes equations, the highly accurate direct simulation Monte-Carlo (DSMC) [3] algorithm is capable to describe such phenomena. Hence, the DSMC algorithm has become a standard tool for modelling rarefied gas flows far away from thermal equilibrium. Since the DSMC algorithm requires modelling of particle collisions, molecular length scales have to be resolved and computational effort for DSMC increases quadratically with decreasing Knudsen numbers. This can be a challenge when simulating multiscale problems that feature a wide range of local Knudsen numbers, like plume expansions or entry flows. To solve this issue a common practice is to couple DSMC with less accurate, but more efficient flow solvers in areas where the resolution of DSMC is not required. As an example, different authors investigated the hybridisation of DSMC and Navier-Stokes solvers [4, 5]. Such a hybridisation becomes challenging because of the fluctuating boundary conditions for the Navier-Stokes solver, caused by the stochastic nature of the DSMC algorithm. Another solution is, to couple DSMC with particle methods, which are feasible to describe the particle motion without modelling particle collisions [6, 7, 8]. An example for such a particle model is the kinetic Fokker-Planck model.

The kinetic Fokker-Planck model was first described by Jenny et al. [8]. The fundamental idea is to approximate the Boltzmann equation by a Fokker-Planck equation in velocity space. Instead of obtaining the particle distribution function by solving the Fokker-Planck equation directly, the random motion of the underlying particles is modelled by an associated random process. This results in a particle handling similar to the DSMC algorithm, which allows for a simple coupling of both methods. Jenny et al. [8] first introduced the *linear model* which leads to an incorrect Prandtl number for monatomic gases in the continuum limit. To fix this issue, different authors invented extensions to the linear model [1, 2, 9, 10]. A popular extension is the *cubic model* by Gorji et al. [1], which has been further extended by methods for simulating gas mixtures [11], polyatomic species [12] and more efficient integration

algorithms [13]. In addition, Gorji and Jenny [14] suggested a scheme to couple the cubic Fokker-Planck algorithm with the DSMC algorithm. Because the H-Theorem is not proven for the cubic model, Gorji et al. [2] suggested the *entropy model*, which satisfies the H-Theorem.

In this work we investigate Gorjis cubic [1] and entropy [2] models in terms of their applicability to the simulation of hypersonic rarefied gas flow. First, we will give a short review of both models. Next, we will analyse the differences of the models compared to standard DSMC. Based on this analysis, we will define a parameter that is capable of characterizing the validity of both models locally in the flow field. Furthermore we will propose a scheme, to use this parameter to efficiently couple the DSMC and Fokker-Planck algorithms. We will test the scheme for one-dimensional shock and two-dimensional cylinder flows. To demonstrate the performance of the proposed scheme, an efficiency study for the cylinder flow test case is performed.

REVIEW OF UTILIZED MODELS

Kinetic Fokker-Planck ansatz

The fundamental concept of the kinetic Fokker-Planck ansatz is to approximate the Boltzmann equation by a Fokker-Planck equation in velocity space. For the monatomic case the Fokker-Planck equation can be written as follows:

$$\frac{\partial f}{\partial t} + v_i \frac{\partial f}{\partial x_i} + \frac{F_i}{m}\frac{\partial f}{\partial v_i} = \underbrace{\frac{\partial}{\partial v_i} A_i f + \frac{\partial^2}{\partial v_k \partial v_k} D^2 f}_{S_{\mathrm{FP}}(f)}. \tag{1}$$

The right hand side of equation (1) defines the Fokker-Planck Operator $S_{\mathrm{FP}}(f)$, where $f(\mathbf{r}, \mathbf{v}, t)$ means the velocity distribution function, defined over the physical space $\mathbf{r}$, velocity space $\mathbf{v}$ and time t. The drift coefficient A_i and diffusion coefficient D are model parameters, $\mathbf{F}$ denotes an external force and m is the particle mass. The underlying particle motion can be described by a set of two stochastic differential equations [8]:

$$\frac{\mathrm{d}\mathbf{x}}{\mathrm{d}t} = \mathbf{v}, \tag{2}$$

$$\frac{\mathrm{d}\mathbf{v}}{\mathrm{d}t} = \mathbf{A} + D\frac{\mathrm{d}\mathbf{W}}{\mathrm{d}t} + \mathbf{F}. \tag{3}$$

Here, $\mathrm{d}\mathbf{W}$ denotes a Wiener process with zero expectation and $\left\langle \mathrm{d}W_i \mathrm{d}W_j \right\rangle = \delta_{ij}$. The basic idea is to simulate an ensemble of particles by integrating equation (2) and (3) for every particle. The particles represent a distribution function that is, in terms of numerical accuracy, identical to the solution of equation (1). Because the Fokker-Planck equation (1) is an approximation to the Boltzmann equation, the kinetic Fokker-Planck algorithm can be regarded as an approximation to the DSMC algorithm.

Cubic model

For the Drift coefficient A_i a cubic ansatz of the thermal particle velocities is chosen [1]:

$$A_i = -\frac{1}{\tau} c_i + \xi_{ij} c_j + \gamma_i \left(c_j c_j - \frac{3 k_{\mathrm{B}} T}{m} \right) + \Lambda \left(c_i c_j c_j - \frac{2 q_i}{\rho} \right). \tag{4}$$

Here $\mathbf{c}$ represents the thermal velocity component, ρ the mass density, T the temperature, $\tau = 2p/\mu$ is a relaxation time, μ the viscosity, p the pressure, q_i the heat flux and $\Lambda = -\frac{1}{\tau \overline{c_i c_i}^4 \rho^3} \left| \det\left(\pi_{ij}\right) \right|$ denotes a constant with the stress tensor π_{ij}. The matrix ξ_{ij} is assumed to be symmetric. The nine model parameters γ_i and ξ_{ij} are chosen such that:

$$\int \mathrm{d}^3\mathbf{c} S_{\mathrm{FP}} \psi = \int \mathrm{d}^3\mathbf{c} S_{\mathrm{Boltz}} \psi \qquad \text{with} \qquad \psi \in \left\{ c_i c_j, c_i c^2 \right\}, \tag{5}$$

where S_{Boltz} is the Boltzmann collision operator. This results in a system of nine linear equations which must be solved in each time step and each grid cell to determine A_i. Note that in the original derivation and in this study the Maxwell

molecule model is used to evaluate the right hand side of equation (5).
For the diffusion coefficient the following simple relation is used:

$$D = \sqrt{\frac{2k_\mathrm{B}T}{\tau m}}. \tag{6}$$

Entropy model

In the entropy model the diffusion coefficient is adjusted, so that the Fokker-Planck equation satisfies the H-Theorem. This is achieved by choosing the following expression for the diffusion coefficient [2]:

$$D = -\frac{\int A_i A_i f \mathrm{d}^3\mathbf{c}}{\int \partial A_j/\partial c_j f \mathrm{d}^3\mathbf{c}}. \tag{7}$$

For the drift coefficient a similar ansatz than for the cubic model is chosen:

$$A_i = -\frac{1}{\tau}c_i + \xi_{ij}c_j + \gamma_i\left(c_jc_j - \frac{3k_\mathrm{B}T}{m}\right) + \Lambda\left(c_ic_jc_j - \frac{2q_i}{\rho}\right) + 2\gamma_i\left(c_ic_j - \frac{p_{ij}}{\rho}\right). \tag{8}$$

Here p_{ij} denotes the pressure tensor. It can be shown, that equation (7) is linear in γ_i, ξ_{ij} and Λ. Thus, equation (7) can be employed, together with the relation (5) and the following relation:

$$\int \mathrm{d}^3\mathbf{c} S_\mathrm{FP} c^4 = \int \mathrm{d}^3\mathbf{c} S_\mathrm{Boltz} c^4, \tag{9}$$

to form a system of 11 linear equations, which is used to calculate the 11 model parameters γ_i, ξ_{ij}, Λ and D. In strong thermal non-equilibrium equation (7) may give a non-physical negative diffusion coefficient. In this case the relation (9) is neglected and the free parameter Λ is varied by an iterative technique until a positive diffusion is obtained.

Time integration

For the integration of the equation of motions (2) and (3) the scheme presented in [13] is used. For the velocity integration the drift terms (4) and (8) are separated in a linear and a non-linear part. The linear part is integrated analytically, while for the non-linear part a simple Euler scheme is applied. Neglecting the external force $\mathbf{F}$ the solution reads:

$$v_i^{n+1} = \frac{1}{\alpha}\left(c_i^n e^{-\Delta t/\tau} + \left(1 - e^{-\Delta t/\tau}\right)\tau N_i^n + \sqrt{\frac{k_\mathrm{B}T}{m}\left(1 - e^{-2\Delta t/\tau}\right)}\psi_i\right) + U_i^n. \tag{10}$$

The parameter α is used to scale the particle velocities to ensure energy conservation, even when large time steps are used. N_i^n denotes a non-linear expression in the thermal particle velocities, which depends on the expression for the Drift coefficient A_i. For the cubic model one can find:

$$N_i^n = \xi_{ij}c_j + \gamma_i\left(c_jc_j - \frac{3k_\mathrm{B}T}{m}\right) + \Lambda_i\left(c_ic_jc_j - \frac{q_i}{\rho}\right). \tag{11}$$

For the position integration a simple scheme resembling that of DSMC is used:

$$x_i^{n+1} = x_i^n + v_i^n\Delta t. \tag{12}$$

Note that due to the simple position integration scheme (12), the time step should not be much larger than the local mean collision time to avoid errors caused by numerical diffusion. In principle this limitation can be avoided by using more accurate, but also more complex integration schemes [8, 1, 15]. However, in case of hypersonic flows the time step is determined mainly by the Courant-Friedrichs-Lewy (CFL)-Criterion and not by the local mean collision time. Therefore, we do not expect a large increase in the applicable time step for a hypersonic flow simulation, even when using more complex integration schemes.

Numerical parameters

All calculations in this paper are performed using a model of argon. To calculate the viscosity, which is needed to evaluate the Fokker-Planck relaxation time τ, the variable hard sphere (VHS)-power law is applied:

$$\mu = \mu_{\text{ref}} \cdot \left(\frac{T}{T_{\text{ref}}} \right)^{\omega} . \tag{13}$$

The production terms (5) and (9) are evaluated using the Maxwell molecule model. To be consistent $\omega = 1$ is applied for all simulations, with $\mu_{\text{ref}} = 2.64 \cdot 10^{-5}$ Pa · s and $T_{\text{ref}} = 273$ K. For the DSMC calculations the VHS-collision model is used with $d_{\text{ref}} = 4.11 \cdot 10^{-10}$ m as reference diameter. For simplicity, the mean free path λ is calculated using the expression for a VHS gas:

$$\lambda = \frac{1}{\sqrt{2}\pi n d_{\text{ref}}^2 \frac{T}{T_{\text{ref}}}^{\omega-1}}, \tag{14}$$

where n denotes the number density and T the temperature. In the following discussion, the indexed values λ_1 and λ_2 refer to the mean free paths based on the flow conditions before and after the shock.

VALIDITY OF KINETIC FOKKER-PLANCK MODELS

The kinetic Fokker-Planck algorithm reproduces a particle distribution function as described by the Fokker-Planck equation. Similarly the DSMC algorithm reproduces a distribution function as described by the Boltzmann equation. Therefore, to investigate differences between the two methods we will search for differences between both equations. By multiplying Boltzmann and Fokker-Planck equation with trace-free velocity products $mc^{2a}c_{<i_1}c_{i_2}\dots c_{i_n>}$ and integrating over the velocity space, we can transform both equations in an equivalent set of moment equations [16]. The solution reads:

$$\frac{\mathrm{D}u^a_{i_1 i_2 \dots i_n}}{\mathrm{d}t} + \dots = P^a_{i_1 i_2 \dots i_n}, \tag{15}$$

in case of the Boltzmann equation and:

$$\frac{\mathrm{D}u^a_{i_1 i_2 \dots i_n}}{\mathrm{d}t} + \dots = K^a_{i_1 i_2 \dots i_n}, \tag{16}$$

in case of the Fokker-Planck equation. Here $u^a_{i_1 i_2 \dots i_n}$ denotes a trace-free moment and $P^a_{i_1 i_2 \dots i_n}$ ($K^a_{i_1 i_2 \dots i_n}$) a Boltzmann (Fokker-Planck) production term:

$$u^a_{i_1 i_2 \dots i_n} \equiv m \int c^{2a} c_{<i_1} c_{i_2} \dots c_{i_n>} f \mathrm{d}^3 C, \tag{17}$$

$$P^a_{i_1 i_2 \dots i_n} \equiv m \int c^{2a} c_{<i_1} c_{i_2} \dots c_{i_n>} S_{\text{Boltz}}(f) \mathrm{d}^3 C, \tag{18}$$

$$K^a_{i_1 i_2 \dots i_n} \equiv m \int c^{2a} c_{<i_1} c_{i_2} \dots c_{i_n>} S_{\text{FP}}(f) \mathrm{d}^3 C. \tag{19}$$

The left sides of equations (15) and (16) are identical. Because of the mass, momentum and energy conservation of the Fokker-Planck operator and the relationships (5) and (9) we have $P^a_{i_1 i_2 \dots i_n} = K^a_{i_1 i_2 \dots i_n}$ for the cubic model when $(a, n) \in \{(0,0), (1,0), (0,1), (0,2), (1,1)\}$ and for the entropy model when $(a, n) \in \{(0,0), (1,0), (0,1), (0,2), (1,1), (2,0)\}$. In all other cases we have $P^a_{i_1 i_2 \dots i_n} \neq K^a_{i_1 i_2 \dots i_n}$. So the only differences between equations (15) and (16) are higher order production terms. Conversely this means that differences between higher order production terms can be used to explain discrepancies between kinetic Fokker-Planck and DSMC algorithm. As an example Figure 1 shows density (red) and temperature (blue) extracted from Fokker-Planck and DSMC calculations of one-dimensional shocks with two different upstream Mach numbers. For the small Mach number a good agreement between Fokker-Planck and DSMC results can be observed, while for a higher Mach number, due to the strong thermal non-equilibrium inside the shock, deviations of the Fokker-Planck results from the DSMC results are observed. In particular, the Fokker-Planck algorithm tends to predict a larger shock width, compared to the DSMC algorithm.

Figure 2 shows exemplary a Fokker-Planck production term $\tilde{K}^1_{xx}$ and a Boltzmann production term $\tilde{P}^1_{xx}$ for the same calculations as shown in Figure 1. Compared to K^1_{xx} and P^1_{xx}, the terms $\tilde{K}^1_{xx}$ and $\tilde{P}^1_{xx}$ are scaled with upstream condi-

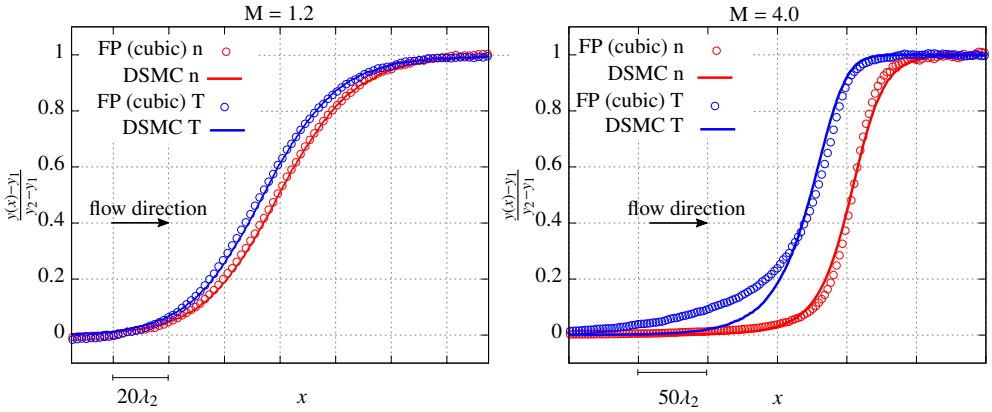

FIGURE 1. Dimensionless temperature and number density over a shock calculated with DSMC (blue) and Fokker-Planck (red). Observe different scales of abscissa.

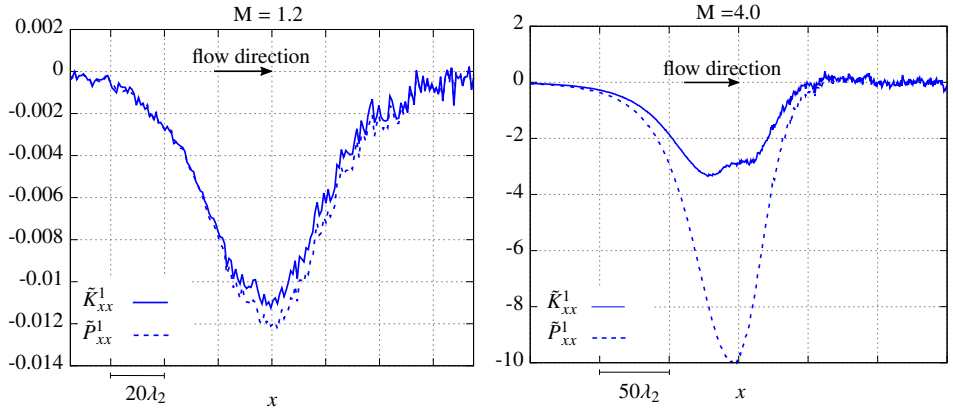

FIGURE 2. Dimensionless production terms $\tilde{P}^1_{xx}$ and $\tilde{K}^1_{xx}$ for two different upstream Mach numbers. Observe different scales of abscissa and ordinate.

tions to achieve dimensionless values. Further, the Fokker-Planck term $\tilde{K}^1_{xx}$ has been calculated from the same DSMC simulation as the Boltzmann term $\tilde{P}^1_{xx}$. This ensures, that differences between the results do not arise because of different distribution functions which are used to calculate the terms. For the small Mach number, where Fokker-Planck and DSMC results agree well, only small deviations between both terms can be observed, while for the high Mach number large deviations arise. This observation supports the idea that higher order production terms can be used to characterize the validity of the kinetic Fokker-Planck algorithm.

HYBRID FOKKER-PLANCK DSMC CALCULATION

Non-equilibrium parameter

In this section we define a non-equilibrium parameter which characterizes the validity of the kinetic Fokker-Planck algorithm locally in the flow field. As shown in the last section, the validity of the Fokker-Planck algorithm can be characterized by differences between higher order production terms. Therefore we use differences of production terms to define the non-equilibrium parameter. First we define the dimensionless differences d^1_{ij} by:

$$d^1_{ij} = \frac{1}{\nu\rho u^4}\left(K^1_{ij} - P^1_{ij}\right). \tag{20}$$

Here ν means the local collision frequency, ρ the local mass density and u the average thermal particle speed. Note that in principle arbitrary terms $P^a_{i_1 i_2 \ldots i_n}$ and $K^a_{i_1 i_2 \ldots i_n}$, which are not equalized by the relations (5) and (9) could be used

to define differences $d^a_{i_1 i_2 \ldots i_n}$. The term d^1_{ij} forms a symmetric matrix containing six different elements. In general, all entries could be used to define a non-equilibrium parameter, but for simplicity we only use the diagonal elements. We define as non-equilibrium parameter N_{FP}:

$$N_{\mathrm{FP}} = \left\langle d^1_{xx} \right\rangle_t^2 + \left\langle d^1_{yy} \right\rangle_t^2 + \left\langle d^1_{zz} \right\rangle_t^2. \tag{21}$$

Here $\left\langle \right\rangle_t$ means a time averaging. Let us now summarize some properties of N_{FP}. The parameter is isotropic, it is always positive and most important the parameter vanishes if the Fokker-Planck algorithm is valid. Figure 3 shows exemplary how N_{FP} changes over a shock with upstream Mach number $M = 8.0$. It can be observed, that the parameter becomes

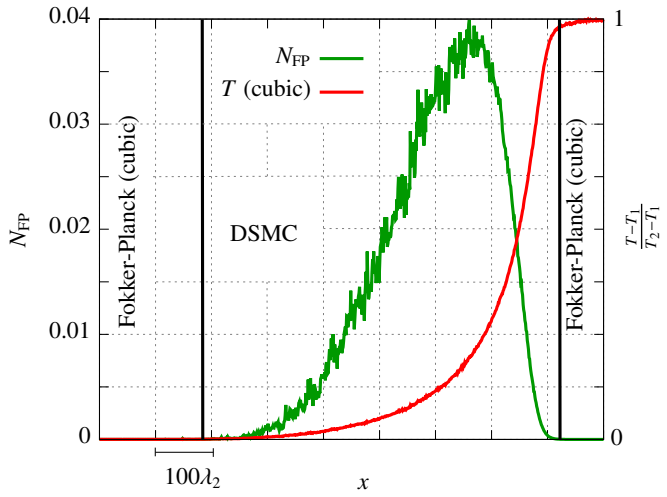

FIGURE 3. Parameter N_{FP} over an $M = 8.0$ shock.

large inside the shock, where the Fokker-Planck ansatz is invalid, and that it vanishes outside the shock, where the Fokker-Planck ansatz is valid again. Based on the parameter the domain can be partitioned into a DSMC and Fokker-Planck area. For this, all cells in which N_{FP} is greater than a certain threshold value $N^{\mathrm{thr}}_{\mathrm{FP}}$ are assigned to the DSMC model, all other cells to the Fokker-Planck model. Note that for the decomposition in Figure 3 and for all further calculations in this paper $N^{\mathrm{thr}}_{\mathrm{FP}} = 5 \cdot 10^{-6}$ is used. This value has been found to be suitable for the test cases in this paper.

Hybridisation schemes

In this section we propose two different schemes for a coupling of DSMC and kinetic Fokker-Planck algorithm.

1st scheme (constant spatial resolution)

1. Perform a Fokker-Planck simulation until a steady state is reached.
2. Perform time averages to calculate N_{FP} by Equation (21).
3. Assign grid cells to the DSMC/Fokker-Planck algorithm based on N_{FP}.
4. Perform a hybrid Fokker-Planck-DSMC simulation till a stationary state is reached.
5. Perform time averages to calculate macroscopic quantities of interest.

2nd scheme (variable spatial resolution)

1. Perform a Fokker-Planck simulation until a steady state is reached.
2. Perform time averages to calculate N_{FP} by Equation (21).
3. Assign grid cells to the DSMC/Fokker-Planck algorithm based on N_{FP}.
4. Adapt DSMC cells to the mean free path.
5. Assign weighting factors Ω to every cell.
6. Perform a hybrid Fokker-Planck-DSMC simulation till a stationary state is reached.
7. Perform time averages to calculate macroscopic quantities of interest.

The first scheme uses the same spatial resolution for the Fokker-Planck and DSMC regions. Thus, the scheme is easy to implement, however it makes no use of the advantages of the Fokker-Planck algorithm which can handle larger grid cell sizes than the DSMC algorithm. Using larger grid cell sizes for the Fokker-Planck region than for the DSMC region introduces a problem with the number of particles per cell. In particular, there will be too few particles in the small DSMC cells or too many particles in the large Fokker-Planck cells. To avoid this problem, cell based weighting factors may be used. As shown schematically in Figure 4, a cell size dependent weighting factor Ω for each cell is

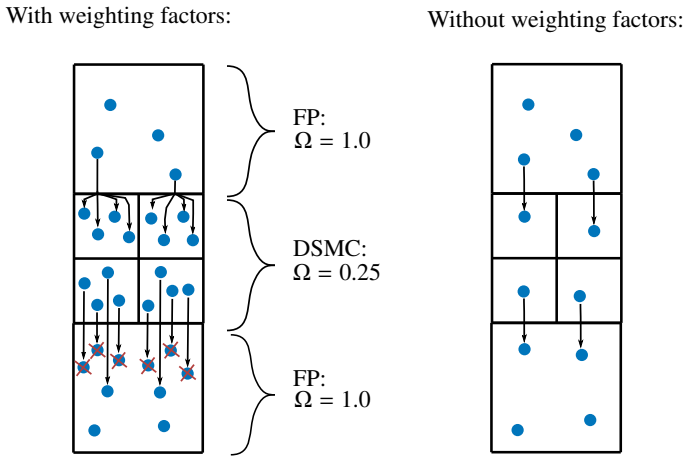

FIGURE 4. Schematically usage of cell based weighting factors.

assigned. When a particle is moving between cells with different weighting factors, the particle is cloned or deleted with a certain probability, depending on the ratio of the weighting factors of the two cells. With a proper selection of the weighting factors the number of particles per cell is independent of the cell size. Thus, the second proposed scheme adapts the DSMC cells to the mean free path and uses cell based weighting factors to achieve a sufficient number of particles per cell.

Hybrid calculations

The first proposed hybridisation scheme is tested for a one-dimensional shock calculation. Figure 5 shows the temperature distribution of a DSMC, Fokker-Planck and hybrid calculation for a shock flow with upstream Mach number $M = 10$. For the DSMC simulation a uniform grid with a cell size smaller than the smallest mean free path in the flow and a time step size smaller than the smallest mean collision time is used. The same resolution is also applied for the hybrid calculations. The scaling factor between real and simulated molecules is adjusted to obtain an average number of 40 particles per cell in the inflow area. While deviations between the DSMC and Fokker-Planck results occur, good

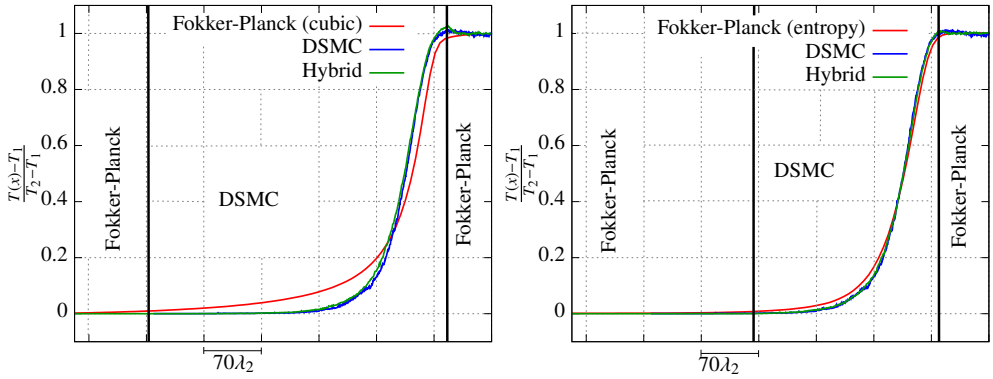

FIGURE 5. Hybrid calculation of a one-dimensional shock with the cubic (left) and entropy model (right).

agreement between the hybrid and DSMC results can be observed. Furthermore, it can be seen that the DSMC region is much smaller when using the entropy model rather than the cubic model. The reason for this is the more accurate prediction of the shock structure by the entropy model. Therefore, for the calculation of more complex test cases the entropy model is recommended.

As more complex test case the two-dimensional hypersonic cylinder flow is investigated. The test case is calculated with the second proposed hybridisation scheme and the entropy model. The cylinder diameter is chosen to $d = 0.3$ m.

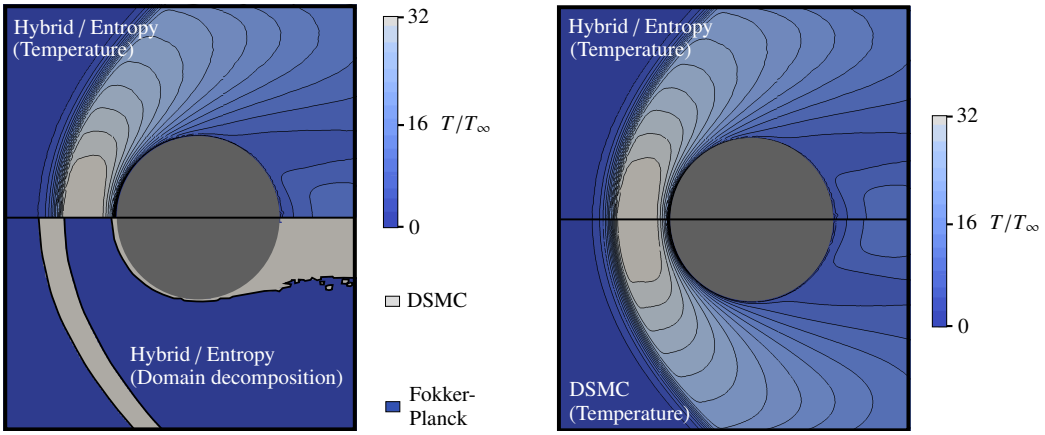

FIGURE 6. Left lower picture: Domain decomposition for a cylinder flow test case. Left upper picture: Temperature contours for the cylinder flow hybrid simulation. Right pictures: Comparison of temperature contours calculated by the hybrid simulation (upper picture) and a reference DSMC simulation (lower picture).

The domain length is set to be $2d$ in free stream direction and $3.3d$ perpendicular to it. The upstream conditions are adjusted to achieve a Mach number of $M = 10$ and a Knudsen number of $Kn = 0.005$. The particle-wall interaction is assumed to be fully diffusive with a wall temperature of $T_W = 500$K. The test case is taken from [17], only the number density is adjusted to achieve the different Knudsen number. For the reference DSMC simulation the computational

grid is adapted to the mean free path, the time step size is chosen to be smaller than the smallest mean collision time in the flow and the scaling factor between the number of real to simulated molecules is chosen so that in the inflow area a number of 15 particles per cell is obtained. For the hybrid calculation the domain is initially divided in a 100×200 uniform grid and the same time step size than for the DSMC simulation is applied. The scaling factor between the number of real to simulated molecules is chosen to obtain an number of 45 particles per cell in the inflow area. For the Fokker-Planck cells a constant weighting factor of $\Omega_{FP} = 1$ is applied, while for the DSMC cells $\Omega_{DSMC} = 0.01$ is chosen. The left lower part of Figure 6 shows the decomposition of the flow field into a DSMC and a Fokker-Planck domain based on the proposed parameter N_{FP}. The DSMC algorithm is applied to simulate the shock, the boundary layer and the wake region. Even though the parameter N_{FP} was originally defined based on shock calculations, it seems to be able to detect invalidation of the Fokker-Planck algorithm because of different physical processes. The right side of Figure 6 shows a direct comparison between hybrid and DSMC results. A very good agreement between both results can be observed.

Efficiency study

First of all we consider the reasons why the Fokker-Planck algorithm holds the potential to be more efficient than the DSMC algorithm when the Knudsen number is small. In a DSMC calculation particle collision must be modelled, whereas in a Fokker-Planck calculation, no collisions need to be modelled. Thus, when changing the number of particles per cell by changing the number density, the computational time for updating particle velocities is for a DSMC calculation quadratic and for a Fokker-Planck calculation linear in the number of particles. As shown schematically

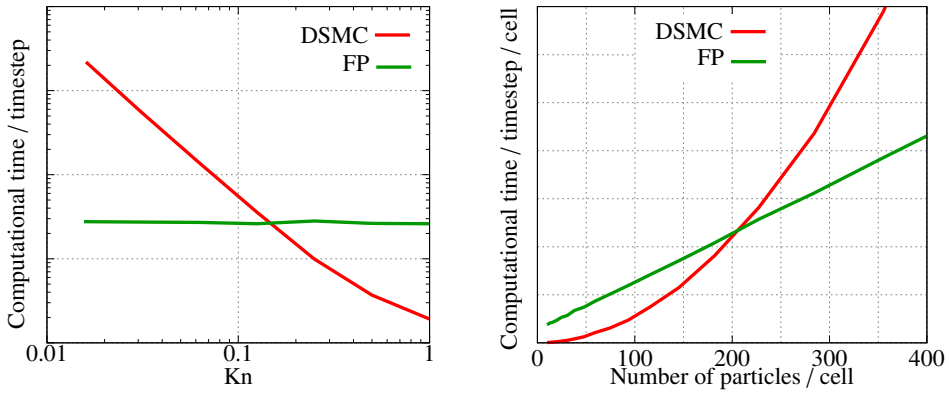

FIGURE 7. Computational time by changing the number density (right) and Knudsen number (left) for a DSMC and Fokker-Planck calculation.

on the right side of Figure 7, DSMC is more efficient than Fokker-Planck for fewer particles per cell. The reason for this is that the cubic and entropy Fokker-Planck models always require the solution of a linear system of equations, regardless of the number of particles per cell. However at a certain number of particles per cell Fokker-Planck will be more efficient than DSMC. For praticle applications this means, that an efficiency benefit can be achieved by using the Fokker-Planck algorithm in cells with a high density, where the DSMC algorithm would be underresolved. Further a DSMC simulations needs to resolve the mean free path. Thus, depending on the dimension of the problem, the computational time for DSMC is quadratic or cubic with the inverse Knudsen number. By a Fokker-Planck simulation there are no such requirements. As shown schematically on the left side of Figure 7, for high Knudsen numbers DSMC is again more efficient than Fokker-Planck. When the Knudsen number becomes smaller than a certain value, Fokker-Planck will become more efficient. This is exactly the mechanism which is exploited by the proposed *2nd hybridisation scheme*. In addition, a DSMC simulation needs to resolve the mean collision time. Especially when its required to calculate a given time interval, many time steps might be needed when using the DSMC algorithm. In contrast to that, under the requirement that accurate time integration schemes are used to solve the equations of motion (2) and (3), the Fokker-Planck algorithm can use arbitrary time step sizes.

Figure 8 shows the relative computational time which was needed by the different algorithms to calculate the hypersonic cylinder flow test case, described in the last section. Furthermore it is shown how the computational time is distributed to the different parts of the algorithm. Here *other actions* summarizes the time which was needed for

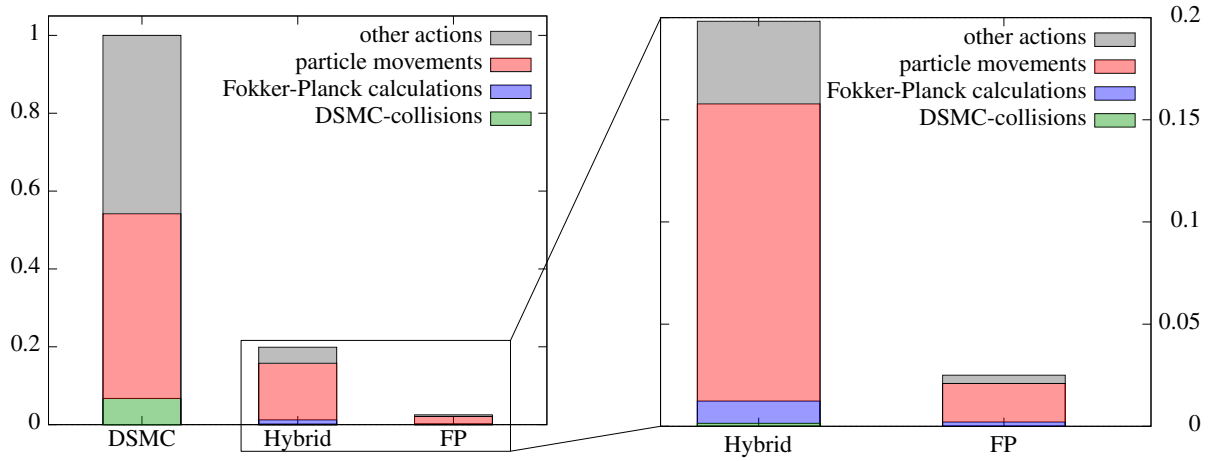

FIGURE 8. Computational time needed by the cylinder flow test case.

tasks like performing time averages or adapting grid cells. The DSMC simulation is the most expensive calculation. The hybrid simulation is roughly five times and the pure Fokker-Planck simulation 40 times faster than the DSMC simulation. Further it should be noted, that only a small amount of time is needed to update the particle velocities by modelling DSMC collisions or performing the Fokker-Planck algorithm, whereas the most amount of time is needed to move the particles through the domain. This observations are contrary to results of other authors who found a fraction of $20 - 35\%$ for the collision time compared to the total simulation time in DSMC simulations of low Knudsen number flows [18] . However, the problem under consideration features a hypersonic flow velocity which causes the time step size to be determined mainly by the CFL-Criterion and not by the local mean collision time. In such a case, the most computational task is the movement of the particles and not the calculation of the collision process. Similar obersvations have been made by Padilla [19] who found a fraction of only $\approx 5\%$ for the collision time compared to the total simulation time in DSMC simulations of a hypersonic flow over a flat plate. For this special test case, we would therefore not expect a large gain in the overall computational time, by improving the Fokker-Planck algorithm.

CONCLUSION

In this study the cubic [1] and entropy [2] Fokker-Planck models are investigated concerning their applicability to simulate strong shock flows. A comparison between Fokker-Planck and the Boltzmann operator shows that deviations from the DSMC algorithm can be attributed to differences in higher order Fokker-Planck and Boltzmann production terms. Based on that, a non-equilibrium parameter is introduced which is able to characterize the validity of the kinetic Fokker-Planck algorithm locally in the flow field. Using this parameter a hybridisation scheme is proposed for efficiently coupling of the kinetic Fokker-Planck and DSMC algorithm. A efficiency study shows, that the proposed hybridisation scheme is five times faster than a pure DSMC calculation for a hypersonic cylinder flow test case.

REFERENCES

[1] M. H. Gorji, M. Torrilhon, and P. Jenny, Journal of Fluid Mechanics **80**, 574–601 (2011).

[2] M. H. Gorji and M. Torillhon, "A Fokker-Planck model of hard sphere gases based on H-theorem," in *Proceedings of the 30th International Symposium on Rarefied Gas Dynamics*, AIP Conference Proceedings 1786 (American Institute of Physics, 2016) p. 090001.

[3] G. A. Bird, *Molecular Gas Dynamics and the Direct Simulation of Gas Flows* (Clarendon Press, Oxford, 1994).

[4] D. Wadsworth and D. Erwin, "One-dimensional hybrid continuum/particle simulation approach for rarefied hypersonic flows," in *5th Joint Thermophysics and Heat Transfer Conference* (American Institute of Aeronautics and Astronautics, 1990) p. 1690.

[5] T. E. Schwartzentruber, L. C. Scalabrin, and I. D. Boyd, Journal of Computational Physics **225**, 1159–1174 (2007).
[6] J. Burt and I. Boyd, Journal of Computational Physics **227**, 4653–4670 (2008).
[7] M. N. Macrossan, "A particle-only hybrid method for near-continuum flows," in *AIP Conference Proceedings*, Vol. 585 (AIP, 2001), pp. 388–395.
[8] P. Jenny, M. Torrilhon, and S. Heinz, Journal of Computational Physics **229**, 1077–1098 (2010).
[9] J. Mathiaud and L. Mieussens, Journal of Statistical Physics **162**, 397–414 (2015).
[10] S. K. Singh and S. Ansumali, Physical Review E **91**, p. 033303 (2015).
[11] H. Gorji and P. Jenny, Journal of Physics: Conference Series **362**, p. 012042 (2012).
[12] M. H. Gorji and P. Jenny, Physics of Fluids **25**, p. 062002 (2013).
[13] M. H. Gorji and P. Jenny, Journal of Computational Physics **262**, 325–343 (2014).
[14] M. H. Gorji and P. Jenny, Journal of Computational Physics **287**, 110–129 (2015).
[15] F. Fei, Z. Liu, J. Zhang, and C. Zheng, Communications in Computational Physics **22**, 338–374 (2017).
[16] H. Struchtrup, *Macroscopic Transport Equations for Rarefied Gas Flow* (Springer Berlin Heidelberg, 2005).
[17] A. J. Lofthouse, L. C. Scalabrin, and I. D. Boyd, Journal of Thermophysics and Heat Transfer **22**, 38–49 (2008).
[18] A. Amiri-Jaghargh, E. Roohi, H. Niazmand, and S. Stefanov, Journal of Heat Transfer **135**, 101008–2 (2013).
[19] J. F. Padilla, "Comparison of DAC and MONACO DSMC codes with flat plate simulation," Tech. Rep. 216835 (NASA, 2010).